

Scattering of an attractive Bose-Einstein condensate from a barrier: Formation of quantum superposition states

Alexej I. Streltsov, Ofir E. Alon, and Lorenz S. Cederbaum
*Theoretische Chemie, Physikalisch-Chemisches Institut, Universität Heidelberg,
 Im Neuenheimer Feld 229, D-69120 Heidelberg, Germany*
 (Received 18 December 2008; published 19 October 2009)

Scattering in one dimension of an attractive ultracold bosonic cloud from a barrier can lead to the formation of two nonoverlapping clouds. Once formed, the clouds travel with constant velocity, in general different in magnitude from that of the incoming cloud, and do not disperse. The phenomenon and its mechanism—transformation of kinetic energy to internal energy of the scattered cloud—are obtained by solving the time-dependent many-boson Schrödinger equation. The analysis of the wave function shows that the object formed corresponds to a quantum superposition state of two distinct wave packets traveling through real space.

DOI: [10.1103/PhysRevA.80.043616](https://doi.org/10.1103/PhysRevA.80.043616)

PACS number(s): 03.75.Kk, 03.65.–w, 03.75.Nt, 05.30.Jp

I. INTRODUCTION

Quantum superposition states are subject of numerous studies in different branches of physics, touching upon fundamental problems of quantum mechanics [1–4]. Practical realization of these states, in particular for larger systems, is an experimental challenge because these states are fragile being sensitive to internal interactions, experimental noise, and other imperfections. In the context of ultracold Bose gases several propositions have been made to creating superposition states prepared in a trap. Side by side, much attention has been paid to dynamics of low-dimensional attractive Bose gases both experimentally and theoretically [12–19]. Bridging these two subjects of intense activity, we report below on a completely different physical mechanism to generate superposition states and a fundamentally new many-body phenomenon in low-dimensional attractive Bose gases accessible within present experimental setups. Explicitly, we demonstrate by solving the time-dependent many-boson Schrödinger equation, that scattering of a one-dimensional attractive ultracold bosonic cloud from a barrier can lead to the formation of two nonoverlapping clouds. Once formed, the clouds travel with constant velocity, in general different in magnitude from that of the incoming cloud, and do not disperse. The analysis of the obtained time-dependent wave function shows that it describes a quantum superposition state of two distinct wave packets traveling through real space. The structure of the paper is as follows. We open in Sec. II by reporting on the splitting phenomenon of a low-dimensional attractive condensate when scattered from a potential barrier, unveiled by accurate many-body numerical “experiments.” Then, in Sec. III, a detailed analysis of the splitting phenomenon along with the many-boson wave function of the system is performed, proving that the split object is a quantum superposition state. Section IV presents a discussion of the splitting phenomenon, in particular in comparison to other split objects reported in the literature. Finally, we conclude in Sec. V.

II. PHENOMENON: SPLITTING BY SCATTERING

In the present work, we start from an attractive cloud made of $N=100$ bosons, prepared in the ground state and

localized around the origin. To scatter it from a potential barrier we add some initial velocity to the cloud. We use a Gaussian barrier placed quite apart from the initial wave packet. The time-dependent many-boson Schrödinger equation is solved as discussed below for a fixed barrier height and several different barrier widths. The results of these scattering “experiments” are plotted in Fig. 1; the width of the barrier increases from left to right panels. It is clearly seen that the wave-packet dynamics very much depends on the barrier width. In the left panel the wave packet overcomes the barrier and continues to propagate further forward without dispersion and losses. In the right panel, the wave packet is reflected from the barrier and continues to propagate backward without dispersion and losses. The middle panel shows fundamentally different and unexpected dynamics: the initial wave packet is split into two parts. One of them is transmitted through the barrier and another one is reflected by the barrier. After their formation, each of the parts has its own constant velocity, here smaller in magnitude from that of the incoming cloud, and continues to propagate without dispersion. It will be shown below that this split object corresponds to a quantum superposition state.

III. ANALYSIS OF THE SPLITTING PHENOMENON AND ITS MANY-BOSON WAVE FUNCTION

We recall that in the standard textbook-problem of scattering a single-particle wave packet from a barrier there are generally transmitted *and* reflected waves. It is thus anticipated that, due to the mutual attraction between the particles, the ultracold cloud being scattered from a barrier is either totally transmitted or totally reflected depending on the barrier’s parameters and initial kinetic energy. The left and right panels of Fig. 1 represent this expected behavior, while in the middle scenario this picture is violated. To understand this phenomenon, we begin with the energetics of the simulated scattering processes. Throughout this work, we use dimensionless units for length, time, and energy, which are readily arrived at by dividing the Hamiltonian by $\frac{\hbar^2}{mL^2}$, where m is the mass of a boson and L is a convenient length scale, say the size of the atomic cloud. The one-body Hamiltonian then

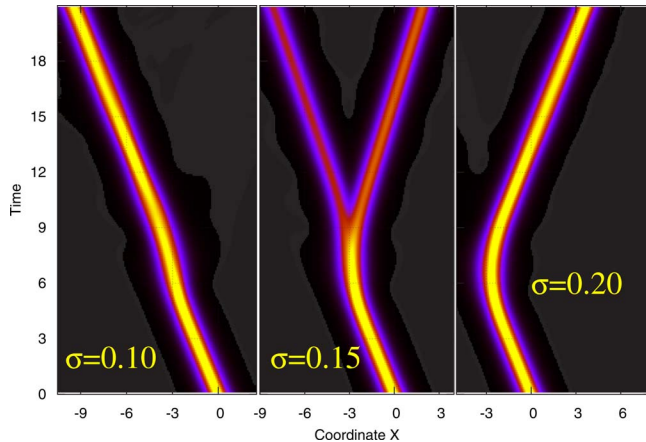


FIG. 1. (Color online). Scattering of a solitonic wave packet initially located at $x=0$ and moving with a constant velocity from Gaussian barriers of different widths σ centered at $x=-3$. Shown is the density as a function of time. Left panel: full transmission case. Right panel: full reflection case. Middle panel: formation of a superposition state of two distinct wave packets traveling through real space with constant velocity smaller in magnitude from that of the incoming cloud. See text for more details. All quantities are dimensionless.

reads: $\hat{h}(x) = -\frac{1}{2} \frac{\partial^2}{\partial x^2} + V_0 \exp[(x+3)^2/2\sigma^2]$. The height of the Gaussian barrier is set to $V_0=0.4$. We employ the commonly used contact interparticle interaction $\lambda_0 \delta(x-x')$ where $\lambda_0 = -0.04$. The energy of the cloud is $E_{GS}/N = -0.66$. The velocity added to the cloud is $v = -0.5$, resulting in kinetic energy of $T_{kin}/N = v^2/2 = 0.125$. Thus, the total energy of the wave-packets $E_{GS} + T_{kin}$ and the barrier height V_0 are the same for the three presented simulations. The only difference between them is the barrier width σ used. In the first, full transmission case $\sigma=0.10$, in the second scenario where the initial packet is split $\sigma=0.15$, and in the third, full-reflection case $\sigma=0.20$. As the initial state is the same for all three scenarios and the barriers' topology and parameters are also quite close to each other, one would have expected that the nature of excitations available for the dynamics in the scattering processes is also quite similar in the three cases.

To better understand the situation, we have to analyze the quantum nature of the propagated wave packets. For that, a brief description of the many-body method used is first needed. To solve the time-dependent many-boson Schrödinger equation for the scattering problem at hand we employ the multiconfigurational time-dependent Hartree method for bosons (MCTDHB) [20]. In the MCTDHB(M) method the time-dependent many-body wave function $\Psi(t)$ is expanded by all time-dependent permanents generated by distributing the N bosons over M time-dependent orbitals. The orbitals as well as the time-dependent expansion coefficients are determined according to Dirac-Frenkel time-dependent variational principle, see [20] for details. We have found that for the scattering scenarios studied here MCTDHB with two orbitals ($M=2$) accurately describes the many-body dynamics. This has been verified by carrying out computations with $M=3$ and even with $M=4$ orbitals. For the sake of comparison, the Gross-Pitaevskii dynamics for a

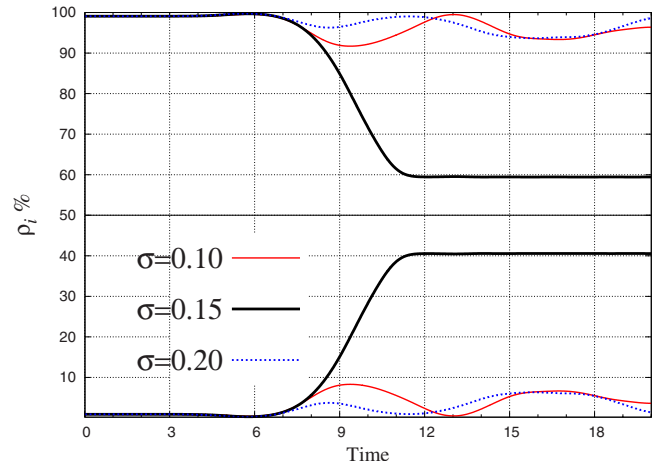


FIG. 2. (Color online). Natural occupation numbers $\rho_i(t)$ in % during the scattering processes of Fig. 1. At $t=0$ all initial wave packets are the same and condensed: $\rho_1(0)=99.1\%$ and $\rho_2(0)=0.9\%$. Until $t=3$ the systems propagate without dispersion, reflecting the solitonic character of the initial wave packet. In the full reflection ($\sigma=0.10$) and transmission ($\sigma=0.20$) cases the systems remain mainly condensed all the time. In the split case ($\sigma=0.15$), after interaction with the barrier, the system evolves into a twofold fragmented state with essentially time-independent occupation numbers $\rho_1=59.5\%$ and $\rho_2=40.5\%$. All quantities are dimensionless.

wide range of parameters has been computed and no splitting phenomenon was found, i.e., the cloud is either transmitted or reflected as a whole. We mention that the famous Gross-Pitaevskii theory is a very particular case of MCTDHB theory where only a single orbital is present ($M=1$).

With the many-boson wave function at hand, we diagonalize at each point in time the reduced one-body density matrix $\rho(x|x';t) = \sum_{i=1}^2 \rho_i(t) \phi_i^*(x',t) \phi_i(x,t)$ for the three scenarios, where the eigenfunctions $\phi_i(x,t)$ are the natural orbitals. In Fig. 2 we plot the obtained eigenvalues (natural occupation numbers) $\rho_i(t)$ as a function of time. These quantities are very useful for a state characterization because according to standard definitions, the system is *condensed* [21] if only one natural orbital is macroscopically occupied and *fragmented* [22] if several natural orbitals have large eigenvalues, i.e., are macroscopically occupied. Accordingly, the initial wave packet is condensed, because almost all the bosons reside in one natural orbital, $\rho_1(0)=99.1\%$. Moreover, till about $t=3$ the systems evolve without changes in the occupation numbers, see Fig. 2. This observation together with the observations seen in Fig. 1 that the systems are moving with constant velocity and without dispersion indicate on the many-body level that the propagating state is a solitonic wave packet. Changes appear when the localized cloud starts to climb up the potential barrier. In the transmission and reflection cases, the interaction of the cloud with the barrier results in a small redistribution of the occupation numbers during and after the collision with the barrier. We conclude that in the full transmission and reflection cases the system remains mainly condensed. In the interaction region, kinetic energy is transformed to potential energy when the cloud is climbing up the barrier and transferred back when

the system is sliding down. In other words, the internal state of the cloud is only slightly affected during the evolutions. In the split case, however, the situation is very different, as one can see from Fig. 2. During the interaction of the wave packet with the barrier, $\rho_2(t)$ grows until it reaches some macroscopic value and saturates around it for long propagation times when the cloud is split. We have found that for the whole range of $0.125 \leq \sigma \leq 0.16$ the splitting phenomenon occurs, with macroscopic occupation of $\rho_2(t)$. We conclude that in the split case, due to interaction of the atomic cloud with the barrier, the system becomes twofold fragmented and stays fragmented afterwards. In this case, the initial kinetic energy is transformed to potential energy which then changes the quantum state of the system. Furthermore, note that the final velocities of the two split clouds are smaller in magnitude from that of the incoming cloud's velocity (see Fig. 1). Because of conservation of total energy, one expects the differences in kinetic energy to be absorbed as internal energy of each of the two split clouds. Our analysis of the many-body wave function indeed shows that this is the case, i.e., that the internal energy of the clouds is larger than that of the initial wave packet.

Let us pose for a moment and summarize our main findings so far. It has been shown that scattering a one-dimensional attractive bosonic cloud in its ground state from a potential barrier can lead to a formation of a twofold fragmented state. Once formed, the fragmented state is dynamically stable, i.e., it retains its properties in time. The mechanism involves transformation of kinetic energy to internal energy of the scattered atomic cloud due to interaction with the barrier. What is the nature of this fragmented state in the attractive Bose system?

To get a deeper insight into the physics of this fragmented-split case, we investigate the many-body structure of the evolving wave packet in more details. In the present study, the total many-body wave function reads $|\Psi(t)\rangle = \sum_{n=0}^N C_n(t) |n, N-n; t\rangle$ where $C_n(t)$ are the expansion coefficients and $|n, N-n; t\rangle$ are the configurations. This ansatz makes the condensed and all possible twofold fragmented states available for the dynamics. The configurations are defined with respect to the natural orbitals and expressed in coordinate space as follows: $\langle x_1, \dots, x_N | n, N-n; t \rangle = \hat{S} \phi_1(x_1, t) \cdots \phi_1(x_n, t) \phi_2(x_{n+1}, t) \cdots \phi_2(x_N, t)$ where \hat{S} is the symmetrization operator. Thus, to prescribe the many-body wave function at a given time it is sufficient to specify the natural orbitals $\phi_1(x, t)$, $\phi_2(x, t)$ and respective expansion coefficients $C_n(t)$. This allows one for a graphical representation and analysis of the whole many-body wave function. In Fig. 3 we analyze the fragmented-split case. The natural orbitals in coordinate space before ($t=0$) and after ($t=20$) the scattering process are plotted in the right panels of Fig. 3. The left part of Fig. 3 depicts the evolution in time of the corresponding expansion coefficients in Fock space, spanned by the $|N, 0\rangle, |N-1, 1\rangle, \dots, |1, N-1\rangle, |0, N\rangle$ configurations (for brevity we do not indicate the dependence of configurations on t here and hereafter). For convenience, the time-dependent probabilities $|C_n(t)|^2$ are plotted.

First we discuss the real-space dynamics of the many-body wave function, i.e., the behavior of the natural orbitals.

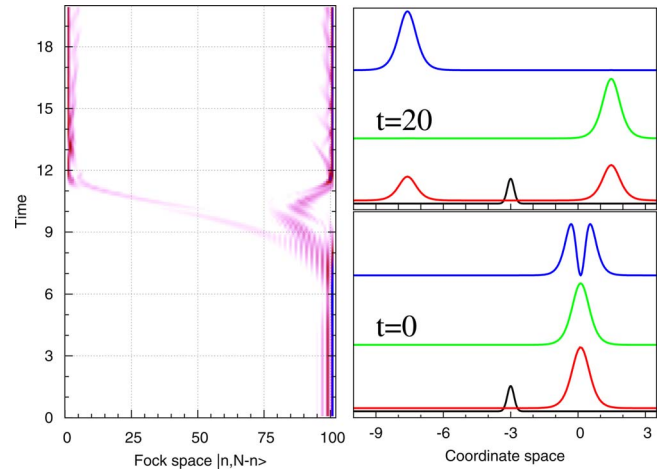


FIG. 3. (Color online). Proof that the split object corresponds to a superposition state of two distinct wave packets. Left panel: evolution of the expansion coefficients in Fock space spanned by the $|N, 0\rangle, |N-1, 1\rangle, \dots, |1, N-1\rangle, |0, N\rangle$ configurations. The probabilities $|C_n(t)|^2$ are plotted as a function of time. The initial wave packet is described essentially by $|N, 0\rangle$. Right upper and lower panels: natural orbitals $|\phi_i(x, t)|^2$ (upper two curves of each of the right panels, in green and blue; normalized to 1) and densities (lower curve of each of the right panels, in red) at $t=0$ and $t=20$. The barrier is also shown (indicated in black and localized around $x=-3$). Mainly the $|N, 0\rangle$ and $|0, N\rangle$ configurations contribute to the split object. All quantities are dimensionless.

As seen in Fig. 3, initially both natural orbitals are localized around the origin. The first natural orbital [$\rho_1(0)=99.1\%$] has no nodes and the *marginally occupied* second natural orbital [$\rho_2(0)=0.9\%$] has one node. After the collision with the barrier and splitting of the cloud, at, e.g., $t=20$, both natural orbitals are localized and have a very similar one-hump-no-node shape, see Fig. 3. It is also important to notice that their profiles (widths) resemble the shape of the primarily occupied natural orbital of the initial state.

Now, we analyze the dynamics of the respective probabilities $|C_n(t)|^2$ in Fock space. As shown in Fig. 3, the initial state is described by a very narrow distribution of the expansion coefficients with maximal contribution provided by the single configuration $|N, 0\rangle$. This picture remains unchanged until $t=3$, where the solitonic many-body wave function starts to interact with the barrier. From Fig. 3 we also see that, during this process, more and more configurations become involved in the dynamics, which is reflected in drastic changes to the overall pattern in Fock space. After the splitting, the pattern of the distribution of the expansion coefficients again becomes relatively simple—there are mainly two dominant configurations, $|N, 0\rangle$ and $|0, N\rangle$, augmented by small contributions from a few respective neighboring configurations.

Let us now combine both observations. The initial wave packet is mainly described by the configuration $|N, 0\rangle$, whereas the split object is formed by a superposition of mainly the $|N, 0\rangle$ and $|0, N\rangle$ configurations. The shapes of the occupied orbitals in *both* cases are very similar and, most importantly, for the split object the orbitals are localized in different regions of space. Remembering that each of $|N, 0\rangle$

and $|0, N\rangle$ is moving with a constant velocity, we can conclude that the split object is a realization of a quantum superposition state, which travels through real space.

IV. DISCUSSION

Several remarks are in order. First, the most important observation is that the split object is formed, and once formed it is stable in time. Second, this split object is not the “perfect” superposition state $\frac{|N,0\rangle+|0,N\rangle}{\sqrt{2}}$. One can see from Fig. 1 that the density of the left split part is smaller than the density of the right part. The quantitative characterization of this “asymmetry” can be obtained from Fig. 2, where we see that the natural occupation numbers saturate at 59.5% and 40.5%, accounting thereby for 59.5% (right part) and 40.5% (left part) of the total density, respectively. Finally, our numerical calculations show that a variety of quantum superposition states can be obtained, depending on the barrier shape, particle number, and interparticle interaction strength.

It is instructive to contrast the superposition states reported here with the fragmented states reported previously in [19] called “fragmentons.” The fragmenton is a dynamically stable fragmented object which is described essentially by a *single* configuration $|N/2, N/2\rangle$ built upon *overlapping delocalized* orbitals [19]. As the fragmenton, the quantum superposition state is also twofold fragmented but, in contrast, a *two-configurational* many-body state formed as a linear combination of $|N,0\rangle$ and $|0,N\rangle$ built upon *nonoverlapping localized* orbitals. Clearly, the quantum superposition states and fragmentons are of a very different but complementary physical nature that can be explained in terms of localization and delocalization in real space and Fock space. The fragmentons appear due to delocalization of the orbitals in real space and localization of configurations in Fock space, while the quantum superposition states are formed due to delocalization of the expansion coefficients in Fock space and localization of the orbitals in real space. An important physical distinction between these two classes of dynamically stable excitations in attractive low-dimensional Bose gases is their energetics. The quantum superposition states lie much lower in energy than fragmentons [19], as is also reflected in the finding that their orbitals are essentially of the same shape as the ground-state orbital (see Fig. 3).

Finally, we discuss experimental observability of the quantum superposition states reported here. As shown in the above detailed analysis, the superposition states are fragmented objects, consisting of two spatially nonoverlapping clouds. This suggests that measuring the first-order correlation function $g^{(1)}(x', x; t) \equiv \rho(x|x'; t) / \sqrt{\rho(x|x; t)\rho(x'|x'; t)}$, which quantifies the system’s degree of spatial coherence, would provide an experimental tool to identify them. Concretely, $g^{(1)}(x', x; t)$ is essentially zero for all x, x' and at all times t , except for the two moving-in-time regimes localized around the diagonal $x=x'$, for which the two nonoverlapping clouds of the quantum superposition state are momentarily localized in space. Furthermore, we have checked and found that disturbing one cloud does not influence the other one. For instance, we scattered the right cloud off a potential wall. The cloud totally bounced back from the wall and the many-

body state remained a superposition state. Due to this robustness, we expect the quantum superposition states in low-dimensional attractive Bose gases reported here to be relatively protected against decoherence.

For completeness, we discuss how can one distinguish the superposition state, which is a fragmented object, from the familiar two-hump soliton with one cloud traveling to the left and the other to the right, which is a condensed object. First of all, the superposition state consists of a linear combination of *two* dominant permanents, $|N,0\rangle$ and $|0,N\rangle$, built upon two localized orbitals. In contrast, the wave function of a two-hump soliton is comprised of only a *single* permanent built upon a single delocalized orbital. It is thus a totally different quantum state of the many-boson system. There are at least three more possibilities to distinguish between superposition states and two-hump solitons. (i) *Correlation functions*. Since the two-hump soliton is a condensed object, its first-order correlation function is flat, i.e., $g^{(1)}(x', x; t) = 1$ for all x, x' and at all times t , in sharp difference to $g^{(1)}(x', x; t)$ of the quantum superposition state discussed above. In fact, all correlation functions of a two-hump soliton are flat, whereas those of quantum superposition states will be structured. (ii) *Energetics*. The total energy of a two-hump soliton is much higher than the total energy employed in our work to generate quantum superposition states. Namely, if one keeps the total energy below the threshold energy for a two-hump soliton formation, the split phenomenon cannot be explained at all in terms of solitons. (iii) *Clouds’ widths*. For N attractive bosons with interaction strength λ_0 , the width $1/\gamma_{\text{superposition}}$ of each of the two clouds in a quantum superposition state is the same as the width of the ground state, i.e., $\gamma_{\text{superposition}} \sim |\lambda_0|(N-1)/2$. In contrast, the width $1/\gamma_{\text{soliton}}$ of each of the two clouds in a two-hump soliton is *twice* as large, i.e., $\gamma_{\text{soliton}} \sim |\lambda_0|(N-1)/4$.

V. CONCLUSIONS

A one-dimensional attractive ultracold bosonic cloud being scattered from a potential barrier can form two nonoverlapping clouds traveling with constant velocity, in general different in magnitude from that of the incoming cloud, and without dispersion. Due to the interaction with the barrier, the initial kinetic energy of the cloud’s wave packet is transformed to potential and internal energies, resulting in formation of two not-exact replicas of the original wave packet augmented by small excitations of the local densities. As a result of the scattering process, the initially condensed state is transformed to a fragmented state. By analyzing the computed time-dependent many-boson wave function it has been shown that the object formed corresponds to a quantum superposition state of two distinct wave packets traveling through real space. The present work demonstrates that low-dimensional attractive Bose gases are rich with novel many-body phenomena. We hope that our work will stimulate experiments.

Note added in proof. Recently, two related works appeared [23,24].

ACKNOWLEDGMENTS

Financial support by DFG is acknowledged.

- [1] C. Monroe *et al.*, *Science* **272**, 1131 (1996).
- [2] M. Brune, E. Hagley, J. Dreyer, X. Maître, A. Maali, C. Wunderlich, J. M. Raimond, and S. Haroche, *Phys. Rev. Lett.* **77**, 4887 (1996).
- [3] J. R. Friedman *et al.*, *Nature (London)* **406**, 43 (2000).
- [4] D. Leibfried *et al.*, *Nature (London)* **438**, 639 (2005).
- [5] J. Ruostekoski, M. J. Collett, R. Graham, and D. F. Walls, *Phys. Rev. A* **57**, 511 (1998).
- [6] J. I. Cirac, M. Lewenstein, K. Mølmer, and P. Zoller, *Phys. Rev. A* **57**, 1208 (1998).
- [7] M. J. Steel and M. J. Collett, *Phys. Rev. A* **57**, 2920 (1998).
- [8] D. Gordon and C. M. Savage, *Phys. Rev. A* **59**, 4623 (1999).
- [9] K. W. Mahmud, J. N. Kutz, and W. P. Reinhardt, *Phys. Rev. A* **66**, 063607 (2002).
- [10] T.-L. Ho and C. V. Ciobanu, *J. Low Temp. Phys.* **135**, 257 (2004).
- [11] Y. P. Huang and M. G. Moore, *Phys. Rev. A* **73**, 023606 (2006).
- [12] P. A. Ruprecht, M. J. Holland, K. Burnett, and M. Edwards, *Phys. Rev. A* **51**, 4704 (1995).
- [13] V. M. Pérez-García, H. Michinel, and H. Herrero, *Phys. Rev. A* **57**, 3837 (1998).
- [14] L. Khaykovich *et al.*, *Science* **296**, 1290 (2002).
- [15] K. E. Strecker *et al.*, *Nature (London)* **417**, 150 (2002).
- [16] L. Salasnich, A. Parola, and L. Reatto, *Phys. Rev. Lett.* **91**, 080405 (2003).
- [17] L. D. Carr and J. Brand, *Phys. Rev. Lett.* **92**, 040401 (2004).
- [18] A. D. Martin, C. S. Adams, and S. A. Gardiner, *Phys. Rev. Lett.* **98**, 020402 (2007).
- [19] A. I. Streltsov, O. E. Alon, and L. S. Cederbaum, *Phys. Rev. Lett.* **100**, 130401 (2008).
- [20] A. I. Streltsov, O. E. Alon, and L. S. Cederbaum, *Phys. Rev. Lett.* **99**, 030402 (2007); O. E. Alon, A. I. Streltsov, and L. S. Cederbaum, *Phys. Rev. A* **77**, 033613 (2008).
- [21] O. Penrose and L. Onsager, *Phys. Rev.* **104**, 576 (1956).
- [22] P. Nozières, in *Bose-Einstein Condensation*, edited by A. Griffin, D. W. Snoke, and S. Stringari (Cambridge University Press, Cambridge, England, 1995).
- [23] C. Weiss and Y. Castin, *Phys. Rev. Lett.* **102**, 010403 (2009).
- [24] A. I. Streltsov, O. E. Alon, and L. S. Cederbaum, *J. Phys. B* **42**, 091004 (2009).